Carbohydrate Polymers 88 (2012) 270–281

Contents lists available at SciVerse ScienceDirect

Carbohydrate Polymers

journal homepage: www.elsevier.com/locate/carbpol

Preparation and characterization of IPN composite hydrogels based on polyacrylamide and chitosan and their interaction with ionic dyes

Ecaterina Stela Dragan*, Maria Marinela Perju, Maria Valentina Dinu

"Petru Poni" Institute of Macromolecular Chemistry, Department of Functional Polymers, Grigore Ghica Voda Alley 41A, Iasi 700487, Romania

ARTICLE INFO

Article history:
Received 5 September 2011
Received in revised form 2 November 2011
Accepted 1 December 2011
Available online 13 December 2011

Keywords:
Chitosan
Composite
Cross-linker ratio
Interpenetrating polymer networks
Ionic dyes
Hydrolysis
Swelling ratio

ABSTRACT

Preparation and characterization of some interpenetrating polymer networks (IPN) composite hydrogels based on polyacrylamide (PAAm) and chitosan (CS) are presented in the paper. The reaction variables selected for the preparation of semi-IPN (s-IPN) hydrogels are the ratio of cross-linker (*X*), pH of the reaction mixture, and CS molar mass. The fraction of CS trapped in the s-IPN hydrogels, increased with the increase of the reaction mixture pH from 5 to 6. Full-IPN (d-IPN) hydrogels were prepared by a sequential strategy consisting of the preparation first of s-IPN, followed by the cross-linking of CS with epichlorohydrin, in 2 M NaOH. The partial hydrolysis of the amide groups in PAAm, during the generation of the second network (d-IPN) at high pH, led to the formation of d-IPN hydrogels having a cationic network based on cross-linked CS and an anionic network based on PAAm, which after hydrolysis contains carboxylate groups besides the amide groups. The swelling properties and the interaction with ionic dyes of the d-IPN hydrogels have been strongly influenced by the presence of the two oppositely charged networks. Thus, the s-IPN hydrogel, which contained only positively charged groups, sorbed a higher amount of the anionic dye (Direct Blue 1) than the d-IPN hydrogels. On the other hand, the d-IPN hydrogels sorbed a much higher amount of the cationic dye Methylene Blue than the s-IPN hydrogel.

1. Introduction

Hydrogels are polymer networks able to absorb significant amounts of water without dissolving or losing their structural integrity (Byrne & Salian, 2008). The three-dimensional structure of a swollen hydrogel is maintained by either chemical or physical (hydrogen bonding, van der Waals interaction, hydrophobic interaction, chain entanglements, or ionic complexation) cross-links (Peppas, Hilt, Khademhosseini, & Langer, 2006; Tanaka, Gong, & Osada, 2005). Because of their high water content, hydrogels are similar to a variety of natural living tissues, having widespread applications as biomaterials. Thus, they have found large applicability in reconstructive surgery for artificial organs, tissue engineering, cartilage, muscles, immunoinsulation membranes (Berger et al., 2004; Galaev, 1995; Peppas et al., 2006), etc. Hydrogels are also recommended for controlled delivery of drugs and proteins (Hoare & Kohane, 2008; Kumbar, Soppimath, & Aminabhavi, 2003; Peppas et al., 2006; Reis et al., 2008; Satish, Satish, & Shivakumar, 2006; Muzzarelli, 2009), wastewaters remediation (Jeon, Lei, & Kim, 2008; Yilmaz, Kavakli Akkaş, Şen, & Güven, 2006), or as agricultural products (Abd El-Rehim, 2006; Zohuriaan-Mehr, Omidian, Doroudiani, & Kabiri, 2010).

To enhance the biodegradability as well as the mechanical properties, and to control the diffusion of solutes in hydrogels, multicomponent networks, including biopolymers, as semi- or interpenetrating polymer networks (IPN) have been designed (Agnihotri & Aminabhavi, 2006; Dhara, Nisha, & Chatterji, 1999; Liang, Liu, Huang, & Yam, 2009; Mandal, Kapoor, & Kundu, 2009; Ramesh Babu, Hosamani, & Aminabhavi, 2008; Rodriguez, Romero-Garcia, Ramirez-Vargas, Ledezma-Perez, & Arias-Marin, 2006; Rokhade, Patil, & Aminabhavi, 2007; Varaprasad et al., 2010; Xia, Guo, Song, Zhang, & Zhang, 2005). Semi-IPNs (s-IPN) hydrogels are typically produced in a "single step" by synthesizing a hydrophilic polymer matrix around the preexisting water soluble polymer chains considered as the trapped polymer (Dinu, Perju, & Drăgan, 2011; Myung et al., 2008; Wang, Zhang, & Wang, 2011); alternatively, they are prepared by a selective cross-linking of one polymer in a blend of two polymers (Liang et al., 2009; Myung et al., 2008; Rokhade et al., 2007; Sperling, 1994). Full-IPNs represent an intimate association of two independently cross-linked polymers, at least one of which being cross-linked or synthesized in the presence of the other.

The semi-synthetic polymer chitosan (CS) (Dash, Chiellini, Ottenbrite, & Chiellini, 2011) is a hydrophilic, biocompatible, and biodegradable polymer, which provides to the composite IPN potential for various applications in biomedical, pharmaceutical, and environmental fields (Agnihotri & Aminabhavi, 2006; Berger et al., 2004; Demirel et al., 2006; Kim, Yoon, Kim, & Kim, 2004; Liang

* Corresponding author. Tel.: +40 232 217454; fax: +40 232 211299.
E-mail address: sdragan@icmpp.ro (E.S. Dragan).

0144-8617/$ – see front matter © 2011 Elsevier Ltd. All rights reserved.
doi:10.1016/j.carbpol.2011.12.002

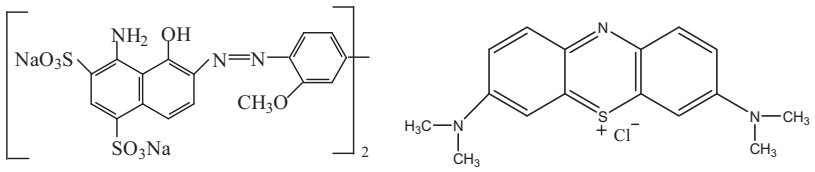

Direct Blue 1 (DB1) Methylene Blue (MB)

Chart 1. Direct Blue 1 (DB1) Methylene Blue (MB).

et al., 2009; Wang, Turhan, & Gunasekaran, 2004; Xia et al., 2005). In this context, the objectives of the paper were: (i) to identify the influence of the cross-linker ratio, pH of the reaction mixture, and CS molar mass on the gel fraction yield and on the fraction of CS trapped in the s-IPN hydrogels having a matrix of poly(acrylamide) (PAAm), and (ii) to prepare amphoteric full-IPN (d-IPN) hydrogels by a sequential strategy consisting of the selective cross-linking of CS trapped in the s-IPN, in alkaline conditions.

As reported in literature, ionic dyes have been used in photodynamic therapy (Hah et al., 2011), as models for drugs in preliminary tests for drug release (Kim & Shin, 2007; Thierry, Winnik, Merhi, Silver, & Tabrizian, 2003) or to test the loading/release of small molecules from multilayer thin films (Chung & Rubner, 2002). Therefore, the interaction of the IPN composite hydrogels with both anionic and cationic dyes has been investigated in the paper as a function of the gel structure to get preliminary indications on the potential applications of the gels in the drug delivery systems.

2. Materials and methods

2.1. Materials

The CS with molar mass of 235 kDa (CS1), purchased from Fluka, and CS with molar mass of 467 kDa (CS2), purchased from Sigma–Aldrich were used as received. The CS molar mass has been calculated from the intrinsic viscosity of CS dissolved in 0.3 M CH_3COOH–0.2 M CH_3COONa (1:1, v/v), at 25 ± 0.1 °C (Gamzazade et al., 1985). Degree of acetylation (DA) of CS was evaluated by infrared spectroscopy (Brugnerotto et al., 2001) by using a Vertex 70 Bruker FTIR spectrometer. Transmission spectra were recorded in KBr pellets. An average value of DA = 15%, resulted from three measurements, has been taken into account for both samples. Acrylamide (AAm, Fluka), N,N′-methylenebisacrylamide (BAAm), ammonium persulfate (APS), N,N,N′,N′-tetramethylethylenediamine (TEMED), all purchased from Sigma–Aldrich, were used as received. Epichlorohydrin (ECH) purchased from Sigma–Aldrich, has been double distilled on KOH before using. Stock solutions of APS and TEMED were prepared by dissolving 0.2 g of APS and 0.625 mL of TEMED each in 25 mL of double distilled water. Stock solutions of BAAm were prepared by dissolving BAAm calculated for a certain cross-linker ratio in 10 mL of distilled water, at 30 °C, under magnetic stirring, and used for hydrogels synthesis after 24 h. Direct Blue 1 (DB1) from Sigma–Aldrich was used after three times recrystallization from an aqueous methanol solution (methanol/water, 70/30, v/v). Methylene Blue (MB) from Sigma–Aldrich was used without purification. The structure of the dyes is presented in Chart 1.

2.2. Preparation of IPN composite hydrogels

Composite hydrogels, based on PAAm and CS, were prepared by free radical cross-linking copolymerization in aqueous medium at 22 °C. The initial concentration of monomers (AAm + BAAm), C_0, has been kept constant in all experiments (5 wt.%). The redox initiator system used consisted of APS and TEMED. The concentrations of APS and TEMED have been constant in all experiments. The cross-linker ratio X (the mole ratio of the cross-linker BAAm to the monomer AAm) varied in the range 1/80–1/20. The feed composition and the samples code of the composite gels are summarized in Table 1.

The general code of semi-IPN composite hydrogels consists of s-IPN followed by 1 or 2, for CS1 or CS2 used as trapped polymer, respectively, and a number with two figures, which represents the mole number of AAm per one mole of BAAm.

2.2.1. Preparation of s-IPN composite hydrogels

The synthesis procedure used in the preparation of s-IPN composite hydrogels is briefly presented below, taking the sample s-IPN1.80 (Table 1) as an example. Typically, 0.4868 g AAm, 6.3 g aqueous solution of CS1 (1 wt.%), obtained by dissolving the flakes in 1 vol.% acetic acid solution and moderate stirring for 48 h, 0.7 mL double distilled water, 1 mL BAAm (0.33 g/25 mL) and 1 mL TEMED

Table 1
The samples code, feed composition, gel fraction yield and percentage of CS removed from the composite gels.

Sample[a]	BAAm:AAm molar ratio	CS			
		Code	Molar mass, M_v (kDa)	GFY[b] (%)	CS removed in s-IPN (wt.%)
PAAm	1/80	–	–	95.5	–
s-IPN1.80	1/80	CS1	235	–	64.33
s-IPN1.80[c]	1/80	CS1	235	91.1	–
s-IPN1.60	1/60	CS1	235	91.1	62.5
s-IPN2.60	1/60	CS2	467	88.8	49.7
s-IPN1.40	1/40	CS1	235	90.1	64.45
s-IPN1.40[c]	1/40	CS1	235	90.4	54.2
s-IPN1.20	1/20	CS1	235	89.6	66.4
s-IPN1.20[c]	1/20	CS1	235	89.4	59.1
s-IPN2.20	1/20	CS2	467	88.2	65.9
d-IPN1.60	1/60	CS1	235	–	–
d-IPN2.60	1/60	CS2	467	–	–

[a] 12.6 wt.% of CS added in the reaction mixture for all composite gels.
[b] Gel fraction yield.
[c] pH adjusted at 6.0.

(0.625 mL/25 mL) were first mixed in a graduated flask of 10 mL. The solution was cooled at 0 °C in ice-water bath, purged with nitrogen gas for 20 min and then, 1 mL of APS stock aqueous solution has been added and the whole mixture has been further stirred about 20 s. Portions of this solution, each 1 mL, were transferred to syringes of 4 mm in diameter; the syringes were sealed, immersed in a thermostated bath at 22 °C, and the polymerization was conducted for one day. After polymerization, the gels were cut into pieces of about 10 mm, and immersed in water for 48 h to wash out any soluble polymers, unreacted monomers and the initiator. Each sample was washed with 40 mL of water five times, and finally the washing solutions were collected all together (about 200 mL). Thereafter, the swollen gel samples were frozen in liquid nitrogen, and freeze dried in a Martin Christ, ALPHA 1-2LD device (24 h, at −57 °C and 0.045 mbar), for 24 h. To evaluate the gel fraction yield (GFY), all s-IPN samples have been further dried under vacuum in the presence of P_2O_5, until the constant weight has been reached. GFY was calculated by Eq. (1):

$$\text{GFY} \quad (\%) = \left(\frac{W_d}{W_m}\right) \times 100 \tag{1}$$

where W_d is the weight of dried sample and W_m is the weight of monomer and cross-linker.

Cross-linked PAAm without CS has been prepared as a reference sample, according to the protocol described above.

2.2.2. Preparation of d-IPN composite hydrogels

The synthesis of d-IPN was performed by the sequential strategy. Thus, the s-IPN synthesized according to Section 2.2.1, cut into pieces of about 10 mm, has been introduced in a flask containing 0.6 mL ECH in 60 mL aqueous solution of 2 M NaOH, before the extraction step, and kept at 22 °C for 24 h, followed by 2 h at 37 °C, to finalize the cross-linking of CS by ECH. The d-IPN has been intensively washed with distilled water up to neutral pH. Dehydration has been performed by repeated washings with methanol until the size of the gel specimens remained constant. The d-IPN samples have been dried in air some hours and than in the oven at room temperature, for 24 h.

2.3. Characterization of s-IPN and d-IPN composite hydrogels

2.3.1. Stability of CS in s-IPN composite hydrogels

Polyelectrolytes give the possibility to quantitatively determining the fraction of polymer, which is effectively trapped in the matrix by the titration of polyelectrolyte, which is removed from the gels by repeated extraction steps at the end of gel preparation. Thus, the concentration of CS, which would leave the composite hydrogel, has been determined by the polyelectrolyte titration of the washing solutions with a standard aqueous solution of poly(ethylene sulfonate) (concentration of 10^{-3} M) by using the particle charge detector PCD 03, Mütek GmbH, Herrsching, Germany. The percentage of CS which left the s-IPN hydrogel by extraction has been calculated with Eq. (2):

$$P_{ex} \quad (\%) = \left(\frac{m}{X}\right) \times 100 \tag{2}$$

where P_{ex} is the percentage of linear polymer removed from the gel, m is the amount of polymer removed from the gel, determined by polyelectrolyte titration, g and X is the theoretical amount of linear polymer contained in the gel, g.

Three values have been averaged.

2.3.2. FTIR

The structure of s-IPN and d-IPN composite hydrogels was investigated by FTIR spectroscopy. The freeze-dried samples have been first frozen in liquid nitrogen, and then broken in a mortar to get the samples as white powder. FTIR spectra were recorded with a Bruker Vertex FTIR spectrometer, resolution 2 cm^{-1}, in the range of 4000–400 cm^{-1} by KBr pellet technique, the amount of the sample being 3–5 mg in each pellet. The structure of s-IPN and d-IPN composite hydrogels after the loading with dyes (contact time 24 h) has been also investigated by FTIR spectroscopy.

2.3.3. DSC

DSC thermograms were obtained using a Pyris Diamond DSC, Perkin Elmer USA. The heating rate was 20 °C min^{-1} and the temperature range was −150 to 300 °C. The samples were prepared as powders in liquid nitrogen by grinding. Constant operating parameters were kept for all the samples in order to obtain comparable data.

2.3.4. Morphological analysis

Surface morphology and internal structure of the dried composite gels were observed by using an Environmental Scanning Electron Microscope (ESEM) type Quanta 200, operating at 20 kV with secondary electrons, in low vacuum mode. The cross-sections of the samples were performed using a sharp blade to revel the internal structures.

2.3.5. Swelling behavior

Swelling properties of composite hydrogels in water were studied using the conventional gravimetric procedure (Kim, La Flamme, & Peppas, 2003, Kim et al., 2004). The dried gels were immersed in water at pH 5.5, and 25 °C. Swollen gels were weighed by an electronic balance, at predetermined intervals, after wiping the excess surface liquid by filter paper. The swelling ratio (SR) was defined by Eq. (3):

$$SR = \left(\frac{W_t - W_d}{W_d}\right), \text{g g}^{-1} \tag{3}$$

where W_d is the weight (g) of the dried sample, and W_t is the weight (g) of the swollen sample, at time t.

2.3.6. Retention capacity for ionic dyes

Adsorption tests of two ionic dyes (DB1 and MB) on the composite hydrogels were carried out using a batch equilibrium procedure. Thus, 0.01 g of dried hydrogel was placed in a flask and contacted with 10 mL of aqueous solution of the dye with a concentration of 2×10^{-5} mol/L, the initial solution pH being 5.5. For kinetic study, the flasks containing the dye solution and the gel were placed in a shaking water bath at 25 °C. After a certain contact duration, hydrogels were filtered off and the residual concentration of the dye remained in the filtrate was measured by the UV–vis spectroscopy at 620 nm for DB1 and at 665 nm for MB. The amount of the dye bound on the composite gels was calculated with Eq. (4):

$$\text{Adsorption} \quad \text{capacity} = \frac{[(C_0 - C)V] \times M_{Dye} \times 10^3}{W}, \text{mg/g} \tag{4}$$

where C_0 and C are the concentrations of the dye in aqueous solution (mol/L) before and after the interaction with dried composite gel, respectively, V is the volume of the aqueous phase (L), and W is the amount of the dried composite gel (g), M_{Dye} is the molar mass of DB1 or MB. For each adsorption experiments, the average of three replicates was reported.

Removal of DB1 from s-IPN hydrogels was performed by repeated treatment with 1 M NaOH, about 48 h, followed by washing at neutral pH. MB has been removed from the d-IPN composite hydrogels by 0.1 M NaOH, about 15 min, followed by washing at neutral pH.

3. Results and discussion

3.1. Stability of CS in s-IPN composite gels

s-IPN composite hydrogels based on PAAm and CS were synthesized in one step by the cross-linking polymerization of AAm in the presence of CS. In the cross-linking copolymerization of AAm with BAAm, the first step was the reaction between APS and TEMED, in which the TEMED catalyzes the decomposition of the persulfate ion to give free radicals species (sulfate and hydroxyl), which initiate the free radical copolymerization. The values of the GFY included in Table 1 demonstrate that the cross-linking polymerization of AAm in this multicomponent system is more complex than the polymerization in the absence of CS (sample PAAm).

As Table 1 shows, the GFY was around (88–91)%, compared with 95.5% found for the cross-linked PAAm, being less influenced by the synthesis parameters than the fraction of CS removed after the synthesis of s-IPN. As can be observed, the percentage of CS removed from the composite gels decreased with the increase of the reaction mixture pH from 5 to 6, because the solubility of CS decreases when the medium pH is closer to its pK_a, and with the increase of CS molar mass.

3.2. Formation of d-IPN composite gels

Generation of the second network was performed by the selective cross-linking of CS with ECH in aqueous solution of NaOH with a concentration of 8 wt.%. It is known that the amide groups in PAAm easily hydrolyze in alkaline conditions generating COO^- groups (Ilavsky, Hrouz, Stejskal, & Bouchal, 1984). The alkaline hydrolysis of PAAm is nonreversible and self-retarded by the effect of the already formed neighboring carboxylate groups (COO^-), which reject the OH^- groups, the rate of hydrolysis decreasing with the increase of the hydrolysis degree. Thus, the simultaneous generation of an anionic network by the partial hydrolysis of PAAm would take place. The mechanism of hydrolysis of amide groups is presented in Scheme 1A.

The formation of the full-IPN composite gels by the selective cross-linking of CS with ECH in alkaline conditions is schematically presented in Scheme 1B. Therefore, the structure of the PAAm matrix in the full-IPN hydrogels would consist of acrylamide, acrylic acid sodium salt, and the cross-linker (BAAm).

To support the hydrolysis of amide groups in the matrix of PAAm which occur during the cross-linking reaction of CS with ECH in alkaline medium, the PAAm having the cross-linker ratio of 1/60, without CS, has been treated with NaOH aqueous solution with concentrations up to 2 M, the contact duration between the PAAm and the alkaline solution being kept constant at 7 h in all experiments. After washing at neutral pH, the values of the SR_{eq} of the gels in water at pH 5.5 and the diameter of gel cylinders in swollen state, D_{sw}, have been measured, their values being plotted in Fig. 1 as a function of the concentration of NaOH aqueous solution used for hydrolysis.

As can be observed, the swelling ratio, SR, dramatically increased from about 27 g/g, measured before the hydrolysis, up to about 800 g/g after 7 h in 0.5 M aqueous solution of NaOH, at 25 °C, and has been less influenced by increasing the concentration of NaOH up to 2.0 M. At the same time, the diameter of the cylinder in swollen state, D_{sw}, increased from about 5 mm, the diameter before the hydrolysis, up to about 17.5 mm after the contact with 0.5 M aqueous solution of NaOH, and has been less influenced by increasing the concentration of NaOH up to 2.0 M. These results support the structural changes which occur in the PAAm matrix during the cross-linking of CS in alkaline conditions, and also show that the concentration of NaOH has a strong influence on the hydrolysis of the amide groups only up to 0.5 M NaOH.

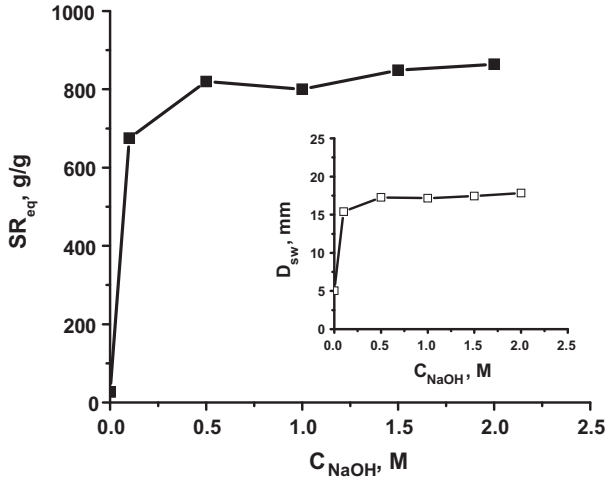

Fig. 1. Swelling ratio, SR, of the PAAm single network having a cross-linker ratio of 1/60, in water at pH 5.5, as a function of the concentration of NaOH aqueous solution used in the hydrolysis of PAAm matrix; plot of the diameter of gel cylinder in swollen state, D_{sw}, as a function of the concentration of NaOH aqueous solution used in the hydrolysis of PAAm matrix is presented in the inset.

3.3. FTIR analysis

The FTIR spectra of one representative sample of s-IPN composite gel (s-IPN1.60), cross-linked PAAm and CS are presented in Fig. 2A.

Because both components of the PAAm/CS composite gels have mainly the characteristic bands in the same regions, it was difficult to assign precisely the peaks found in the spectra of composite gels and to get a clear image about their structural features. Therefore, the spectrum of a physical mixture PAAm:CS, 3:1 (wt/wt) has been also included in Fig. 2A. In the spectrum of s-IPN1.60, some of the characteristic peaks of PAAm were red-shifted, the amide I band was shifted from 1661 cm^{-1}, in the cross-linked PAAm, to 1664 cm^{-1}, and the intense band at 3410 cm^{-1} assigned to the stretching vibration of N—H bond, as well as to hydrogen bonds, shifted to 3436 cm^{-1} in the s-IPN hydrogel. The peak at 1122 cm^{-1}, characteristic to the C—N stretching (secondary amide from BAAm), can be observed in both the spectrum of PAAm and of s-IPN1.60. The peak at 1032 cm^{-1}, assigned to the stretching vibration of the C—O bonds in anhydroglucose ring, can be observed as a shoulder in both the physical mixture of CS with PAAm (1:3) and in the s-IPN1.60 gel.

The peaks at 1082 cm^{-1} and 1032 cm^{-1} in the FTIR spectrum of d-IPN1.60 (Fig. 2B) are characteristic for the skeletal vibration involving the stretching of C—O bonds in anhydroglucose units. Furthermore, the bands at 1718 cm^{-1}, assigned to C=O in carboxylic acids, and at 1404 cm^{-1} assigned to COO^- groups support the hydrolysis of a part of the amide groups to carboxylate groups by the cross-linking of CS with ECH at high pH.

3.4. DSC analysis

The compatibility of the cross-linked PAAm with CS has been examined by DSC. The determination of the glass transition temperature, T_g, represents a very useful tool in order to evaluate the miscibility of a polymer blend. A miscible polymer blend shows a single T_g different from, and, in general, between those of the individual components; on the contrary, an immiscible blend exhibits two different T_g corresponding to those of the single constituents

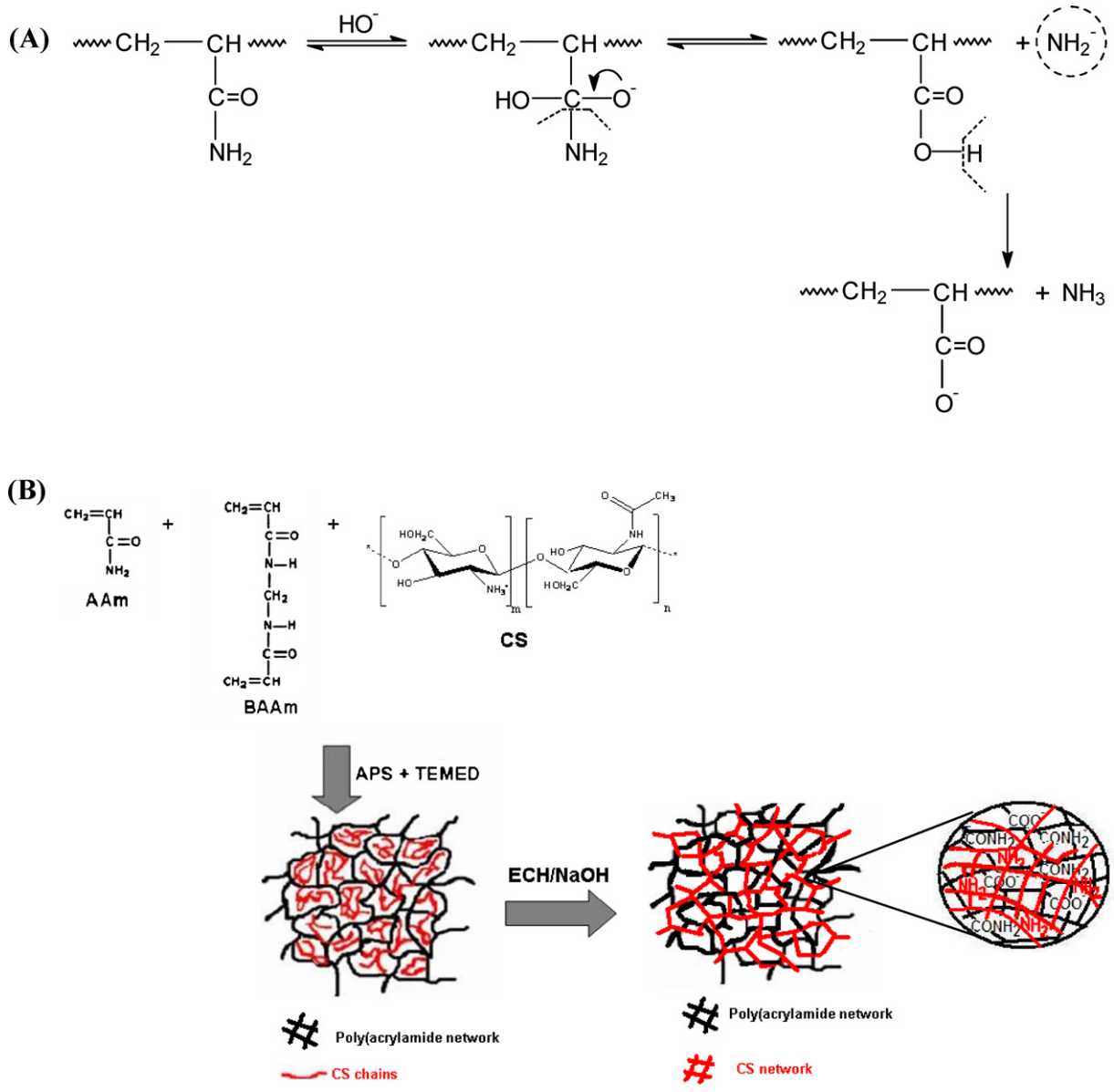

Scheme 1.

(Cascone, Polacco, Lazzeri, & Barbani, 1997). From the typical second scanning thermograms of CS, cross-linked PAAm and s-IPN1.40 it was found that: the cross-linked PAAm showed a single slope change corresponding to the glass transition at 187 °C; CS showed the T_g at a temperature of 207 °C, and the thermogram of s-IPN1.40 hydrogel exhibited a single transition occurring at a temperature located at 189 °C, i.e. between those of the individual components. On the other hand, the thermogram of d-IPN1.40 hydrogel exhibited also a single transition located at a temperature of 295 °C, i.e. a much higher temperature than the s-IPN, and this support the presence of the second network.

3.5. SEM analysis

The morphologies of freeze-dried gel samples were examined by SEM. Fig. 3 shows the microstructure of the s-IPN composite hydrogels as a function of the selected synthesis parameters.

The influence of the cross-linker ratio and of the pH of the synthesis mixture is illustrated in Fig. 3, the trapped polymer being CS1. The SEM images of the freeze-dried hydrogels prepared at pH 5 of the reaction mixture (left images) show a clear influence of the cross-linker ratio on the gel morphology. Thus, the hydrogel formed with a cross-linker ratio of 1/80 has a porous structure, pores with sizes in the range 25–30 μm. It can be also observed that the pore walls of the hydrogels formed with a cross-linker ratio of 1/80 seem not to be strong enough and, therefore, they are more or less fused together. With the increase in the cross-linker ratio, the pores are better defined, the morphology being the best preserved at the highest value of X (X = 1/20), pores with sizes of about 45–50 μm being visible in this case. The right hand images in Fig. 3 show the influence of the pH of the reaction mixture, a higher pH (6) at the same value of X leading to more compact morphologies. The differences have been attributed to the decrease of the ionization degree of CS, when the pH of the reaction mixture was close to its pK_a (6.5, Domard, 1987). Therefore, the CS chains were more rigid and led to more compact walls and smaller pores with sizes in the range 10–15 μm for the s-IPN1.80, and 40–45 μm for the s-IPN1.20. The large polyhedral pores observed in the SEM pictures of s-IPN1.20 hydrogel should be a result of the freeze-drying process of the hydrogels after their preparation. The influence of CS molar

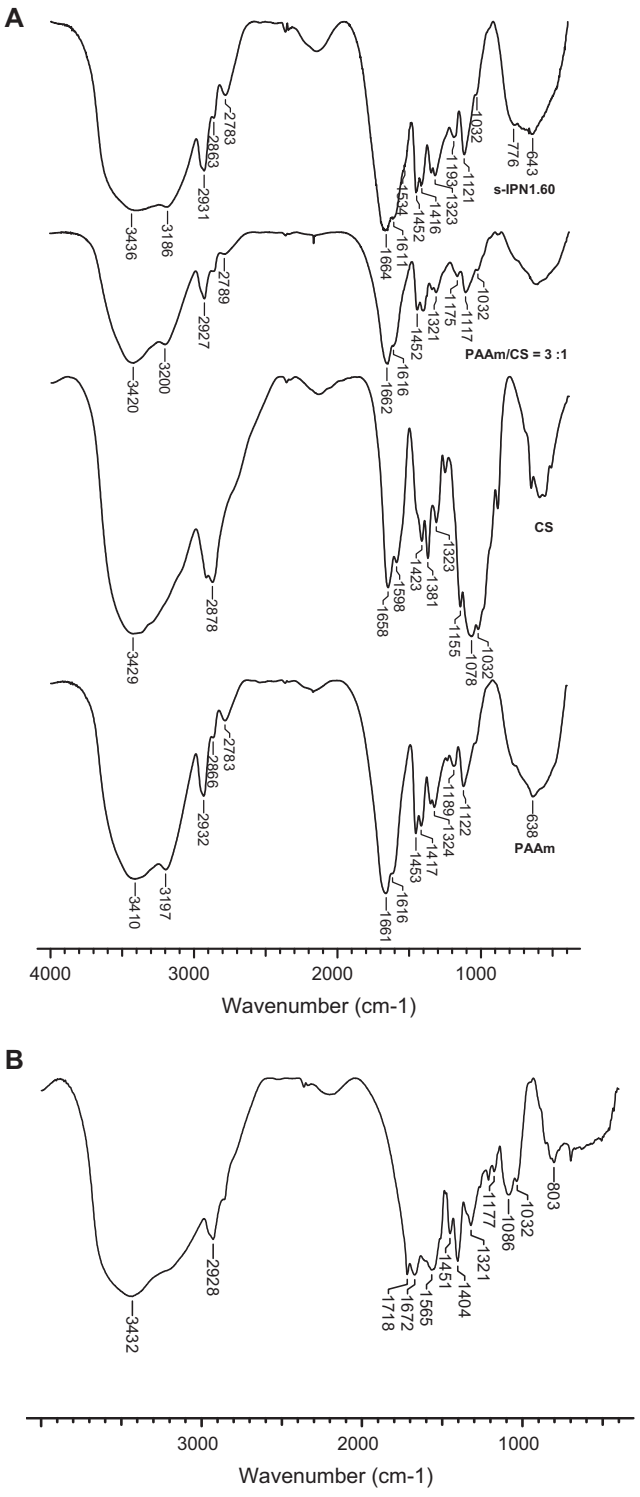

Fig. 2. (A) FTIR spectra of PAAm, CS, physical mixture of PAAm and CS 3:1, and s-IPN1.60; (B) FTIR spectrum of d-IPN2.60.

mass on the morphology of the s-IPN composite gels prepared at pH 5 and a cross-linker ratio of 1/20 showed that with the increase of the CS molar mass a significant decrease of the pore size from 45–50 μm to 5–10 μm occurred.

3.6. Swelling properties of IPN composite hydrogels

The swelling behavior of PAAm/CS composite hydrogels was studied as a function of contact time by measuring the solvent uptake at different intervals. The swelling ratio, *SR*, was calculated by Eq. (3) and the results obtained with four cross-linker ratios are presented in Fig. 4A.

As can be observed from Fig. 4A, the time necessary to attain the equilibrium swollen state starting from the dry state was about 600 min. The values of *SR* were influenced by the cross-linker ratio, the increase of the cross-linker ratio decreasing the *SR* values. At lower cross-link density, the network has a high hydrodynamic free volume to accommodate more of the solvent molecules, thereby increasing matrix swelling (Rokhade et al., 2007). Increasing the cross-linker ratio, the mobility and relaxation of the polymer chains have been hindered, which in turn impedes the mobility of water, lowering the *SR* and the equilibrium water content (Rodriguez et al., 2006). As Fig. 4A shows, the *SR* was higher for the s-IPN prepared with CS2 (s-IPN2.20) than that prepared with CS1 as trapped polymer (s-IPN1.20), at the same cross-linker ratio ($X = 1/20$).

As Fig. 4B shows, the d-IPN1.60 behaves as a superabsorbant hydrogel due to the generation of COO^- groups, its *SR* at equilibrium being 640 g water/g composite, the time necessary to reach the equilibrium swelling being lower than that necessary for the corresponding s-IPN1.60 (400 min compared with 600 min). On the other hand, the *SR* value at equilibrium is lower than that found for the single PAAm network having the same cross-linker ratio, after the contact with NaOH aqueous solution with a concentration of 2 M (864 g/g, Fig. 1). The difference could be attributed to the presence of the second network in d-IPN1.60.

The type of water transport mechanism in hydrogels helps to understand the solute release mechanism (Reis et al., 2008). To evaluate the sorption mechanism of water by the s-IPN and d-IPN composite hydrogels, which are multicomponent systems, the transport of water was analyzed by means of the semiempirical equation proposed by Franson and Peppas (Franson & Peppas, 1983; Kim et al., 2003; Reis et al., 2008), Eq. (5):

$$\frac{M_t}{M_\infty} = kt^n \tag{5}$$

where M_t and M_∞ represent the amount of water uptake at time t and at equilibrium, respectively, k is a characteristic constant of the hydrogel, and n is a characteristic exponent describing the mode of the water transport mechanism.

According to the literature, Eq. (5) is only valid for M_t/M_∞ less than 0.6, because in this portion a linear time dependence of the fractional water uptake for all geometries is obtained (Franson & Peppas, 1983; Kim et al., 2003). Based on the relative rates of penetrant diffusion and polymer chain relaxation, there are three models, which describe the response of hydrophilic polymer networks to the presence of water (Chen, Liu, & Chen, 2009; Kim et al., 2003; Reis et al., 2008): (i) Fickian diffusion ($n = 0.5$), also known as Case I diffusion, occurs when the rate of diffusion is significantly slower than the rate of relaxation of polymer chains; (ii) Case II of transport ($n = 1$) arises when the rate of diffusion is grater that the rate of relaxation of the polymer chains; (iii) non-Fickian or anomalous diffusion ($0.5 < n < 1$) occurs when the rate of diffusion and polymer relaxation are comparable and is connected with the two limiting cases, Case I and Case II. The value of diffusion exponent n and the related transport mechanism depend on the geometry of the samples (Ritger & Peppas, 1987). For a cylinder, n is defined as follows: Fickian diffusion $n < 0.45$ (Case I); $0.45 < n < 0.89$ (Anomalous transport, contribution of Fickian diffusion and polymer chain relaxation); $n = 0.89$ (Case II, transport, contribution of macromolecular relaxation of the polymer chains) (Reis et al., 2008; Ritger & Peppas, 1987).

The portion of the curves with a fractional water uptake M_t/M_∞ less than 0.6 has been analyzed with Eq. (5). The values of M_t/M_∞ as a function of time have been plotted in Fig. 4(C) and (D). The constants n and k were calculated from the slopes and intercepts of the

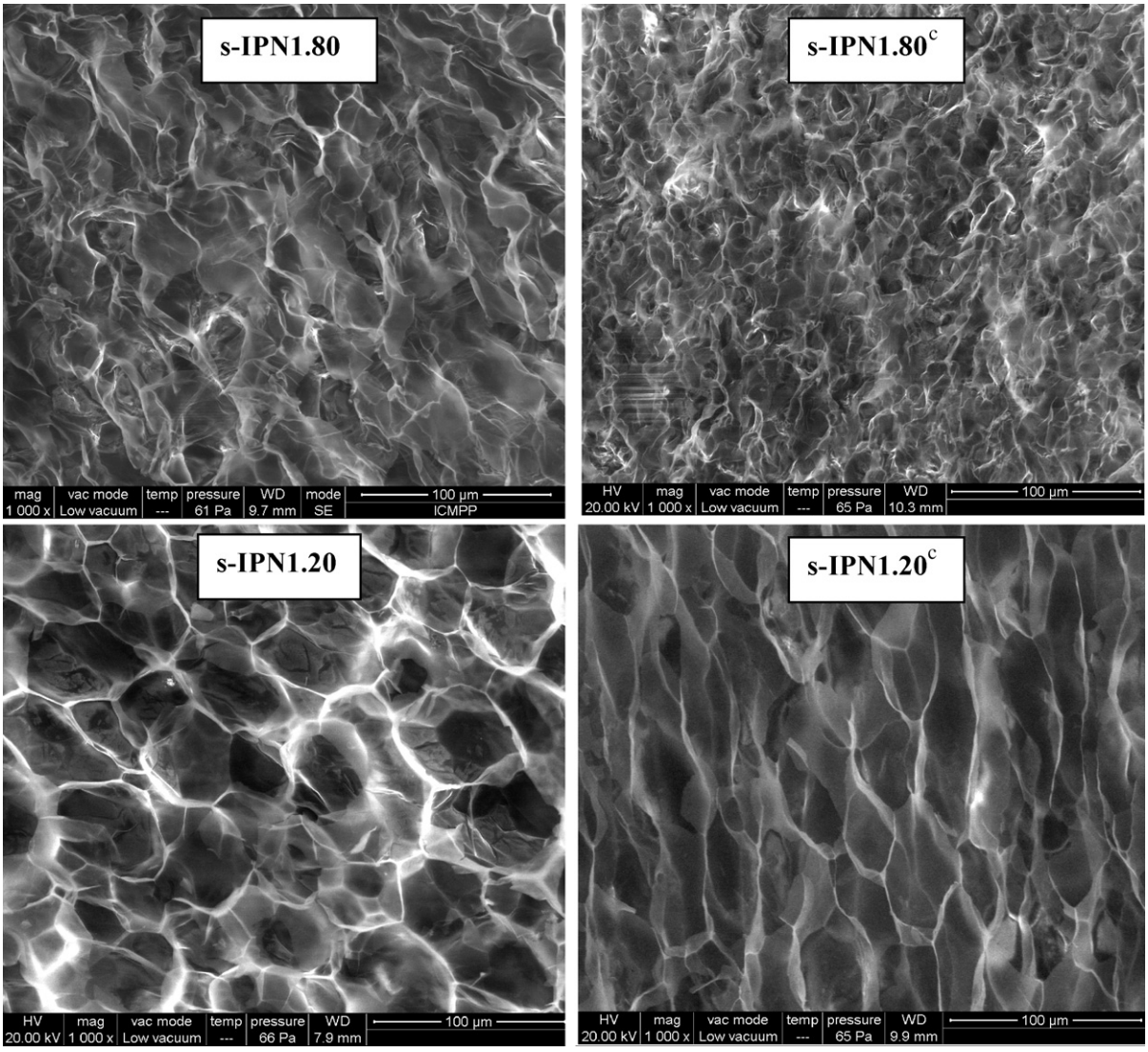

Fig. 3. SEM images of the s-IPN PAAm/CS composite hydrogels prepared at pH 5 (left side), and pH 6 (right side); the scaling bars are 100 μm, Mag = 1000×.

plots of $\log(M_t/M_\infty)$ versus $\log t$ [Eq. (5)] based on the experimental data shown in Fig. 4 (the insets of Fig. 4C and D). The values of n and k are given in Table 2.

As can be observed from Table 2, the values of n calculated for s-IPN PAAm/CS composite hydrogels, with four cross-linker ratios, ranged from 0.29 to 0.42 indicating a Fickian diffusion. The increase of the cross-linking degree led to the slow decrease of the values of n (Table 2). In the case of d-IPN1.60 composite hydrogel, the value of n was 0.38, supporting also a swelling controlled by a Fickian diffusion. The Fickian diffusion mechanism of water molecules into the full-IPN hydrogels can be attributed to the complexity of the multicomponent systems, the presence of two independent networks bearing oppositely charged functional groups (NH_2 groups on the CS network and COO^- on the PAAm network) having a strong influence on the movement of water molecules.

Table 2
Parameters n and k for IPN composite hydrogels as a function of their structure.

Sample	n	k	R^2
s-IPN1.80	0.42 ± 0.015	0.086 ± 0.023	0.997 ± 0.011
s-IPN1.60	0.39 ± 0.02	0.102 ± 0.031	0.995 ± 0.015
s-IPN1.40	0.29 ± 0.025	0.181 ± 0.036	0.989 ± 0.015
s-IPN1.20	0.30 ± 0.02	0.146 ± 0.03	0.992 ± 0.014
s-IPN2.20	0.35 ± 0.015	0.128 ± 0.022	0.997 ± 0.009
d-IPN1.60	0.38 ± 0.01	0.151 ± 0.022	0.998 ± 0.006

3.7. Adsorption of ionic dyes onto IPN PAAm/CS composite gels

3.7.1. FTIR analysis

The analysis of FTIR spectra of the composite gels after the dye adsorption shown in Fig. 5 gives information about the interaction between the dye and the functional groups of the composite gels, as a function of their structure.

Thus, in the spectrum of the s-IPN1.60 loaded with DB1, the characteristic peaks of the dye can be observed as follows: at 1566 cm^{-1}, assigned to the stretching vibrations of —N=N— groups, the characteristic peak for SO_3 group, found in the spectrum of the dye monomer at 1186 cm^{-1}, blue-shifted at 1171 cm^{-1}, the characteristic band of C—S bond at 687 cm^{-1} is red-shifted at 694 cm^{-1}, the band at 1043 cm^{-1} attributed to the C—O—C stretching can be observed as a shoulder at 1040 cm^{-1}, C—H bending vibration in aromatic ring, located at 864 cm^{-1} in the spectrum of the dye monomer is blue shifted at 858 cm^{-1} in the s-IPN1.60 loaded with DB1. The shifts of the wavenumbers show a strong interaction between the protonated primary amino groups in CS and this dye occurred, supported also by the difficult desorption of the dye from the gel

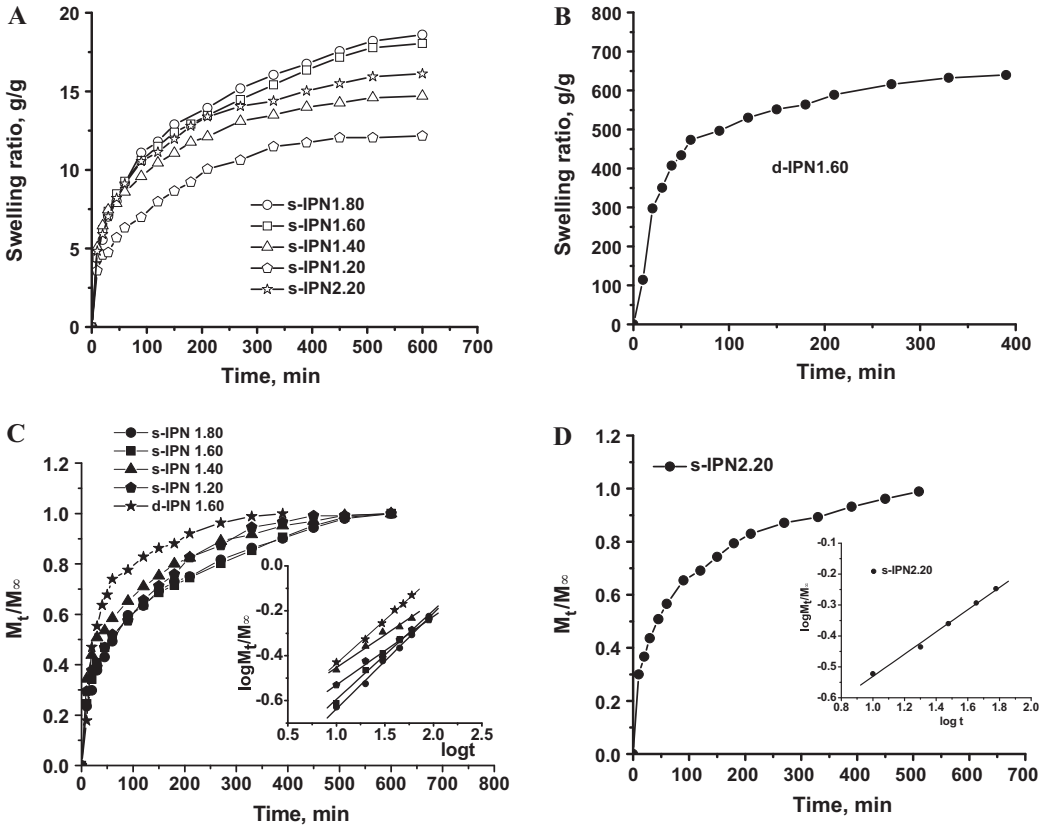

Fig. 4. Swelling ratio as a function of contact time for s-IPN PAAm/CS composite hydrogels with four cross-linker ratios (A) and for d-IPN1.60 (B); M_t/M_∞ as a function of time for PAAm/CS composite hydrogels (C and D).

(repeated treatment with 1 M NaOH, about 48 h). The peak assigned to the stretching vibrations of the C=O bond in amide groups, found at 1664 cm^{-1} in the spectrum of s-IPN1.60, has been shifted at 1668 cm^{-1} after the loading of the gel with DB1, the peak at 1079 cm^{-1}, assigned to the skeletal vibration involving the stretching of C—O bonds in anhydroglucose ring, shows the presence of CS chains.

In the spectrum of the d-IPN1.60 loaded with MB, the characteristic peaks of the dye can be observed as follows: the peak at 1598 cm^{-1}, assigned to the stretching vibration of aromatic ring, the peak at 1566 cm^{-1}, assigned to both the deformation vibrations of the N—H bond, the amide II band, and to the —COO^- groups, the peak at 1403 cm^{-1}, assigned to —COO^- groups, the peak at 887 cm^{-1} assigned to C—H bending vibrations in heterocycle, the shoulder at 666 cm^{-1} assigned to C—S bond vibrations. The peak at 1086 cm^{-1}, is assigned to the skeletal vibration involving the stretching of C—O bonds in anhydroglucose ring. As can be seen, the spectrum of d-IPN1.60 loaded with MB showed no significant shifts of the wavenumbers or appearance of new peaks, indicating that chemical interaction did not occur between the functional groups of the full-IPN composite gel and the cationic dye, the adsorption of MB being physical in nature. Physical adsorption involves small changes of enthalpy, which are not enough for bond breaking (Wan Ngah, Hanafiah, & Yong, 2008).

3.7.2. Adsorption kinetics

The adsorption capacity of the d-IPN1.60 composite hydrogel for the anionic dye, DB1, as a function of contact time, has been compared with that of the s-IPN1.60. The composite gels have been used for the adsorption of DB1 after a previous treatment with HCl 0.1 N (24 h) to generate positive charges on the CS chains. The effect of the contact time on the retention capacity of DB1 on s-IPN1.60 and d-IPN1.60 composite hydrogels is shown in Fig. 6A.

As Fig. 6A shows, the time required to achieve the equilibrium sorption of DB1 at 25 °C was about 120 min for both gels, the difference consisting of the much higher adsorption capacity of s-IPN than d-IPN. Fig. 6B illustrates the sorption kinetics of MB on s-IPN2.60 and d-IPN2.60 composite hydrogels, the time required to achieve the equilibrium sorption of the dye being about 40 min, for both gels. In this case, the amount of the dye sorbed at equilibrium on d-IPN gel was much higher than that sorbed on s-IPN composite gel. The strong interaction of d-IPN with cationic dye supports the presence of anionic charges, COO^-, evidenced in FTIR spectrum of d-IPN2.60 (Fig. 2B). The lower amount of the anionic dye sorbed by s-IPN gel than the amount of MB sorbed by d-IPN gel could be attributed to the much more complex structure of DB1 (Chart 1), an intramolecular interaction between the SO_3^- and NH_2 groups, both positioned in the same benzenic ring, being possible, similar with other anionic dyes (Cestari, Vieira, dos Santos, Mota, & de Almeida, 2004). Thus, these SO_3^- groups are less effective in electrostatic interaction with the NH_3^+ groups of CS.

In order to investigate the controlling mechanism of adsorption process of the s-IPN and d-IPN composite gels against ionic dyes, three kinetic models, i.e. the pseudo-first order model by Lagergren (Eq. (6)), the pseudo-second order model (Ho & McKay, 1998) (Eq. (7)), and the intra-particle diffusion model by Weber and Morris (1963) (Eq. (8)), were used to evaluate the experimental data.

$$\log(q_e - q_t) = \log(q_e) - \frac{k_1}{2.303}t \quad (6)$$

$$\frac{t}{q_t} = \frac{1}{k_2 q_e^2} + \frac{1}{q_e}t \quad (7)$$

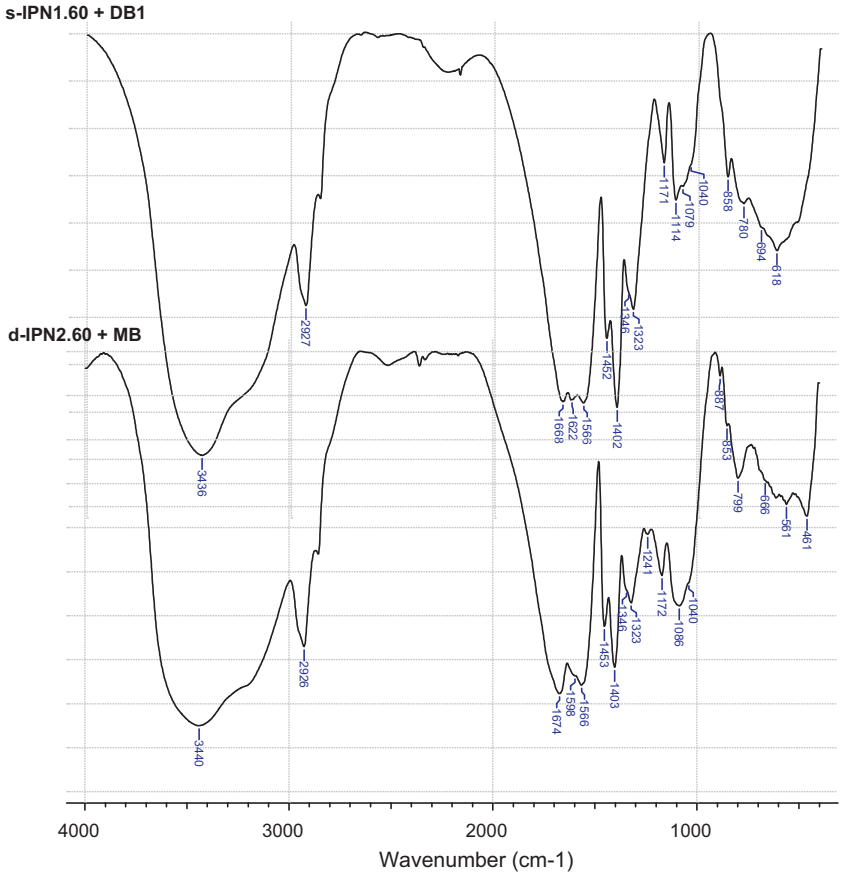

Fig. 5. FTIR spectra of s-IPN1.60 loaded with DB1 and of d-IPN2.60 loaded with MB.

$$q_t = k_{id}t^{0.5} + C_i \quad (8)$$

where q_e and q_t are the amounts of the dye adsorbed at equilibrium (mg/g) and at time t, respectively, k_1 is the rate constant of pseudo-first order kinetic (min^{-1}), k_2 is the rate constant of pseudo-second order kinetic (g/(mg min)), k_{id} is the intra-particle diffusion rate constant (mg/(g $min^{0.5}$)) and C_i is the constant that gives an idea about the thickness of the boundary layer.

The constants corresponding to the pseudo-first order and pseudo-second order models were calculated with an Origin 7.5 program by applying Eq. (6) for the pseudo-first order model, and Eq. (7) for the pseudo-second order model, the values being presented in Table 3.

As Table 3 shows, the theoretical $q_{e,calc}$ values estimated from the pseudo-first order model were very close to the experimental value for both composite hydrogels. On the other hand, d-IPN hydrogel, bearing anionic charges beside the cationic groups, sorbed a small amount of anionic dye. The situation has been reversed in the case of cationic dye, MB, the kinetic of the sorption process being also better described by the pseudo-first order model (Table 3).

The analysis of the kinetic data was performed also by the intra-particle diffusion model (Eq. (8)). If the plot of q_t versus $t^{0.5}$ gives a straight line, which passes through the origin, then the sorption process is controlled only by intra-particle diffusion. However, if the data exhibit multi-linear plots, then two or more steps influence the sorption process. As can be seen from Fig. 7, the adsorption of DB1 and MB onto composite hydrogels was controlled by three different stages: (1) rapid external surface adsorption or instantaneous adsorption stage, (2) gradual adsorption, where intra-particle diffusion is rate-controlling step, and (3) final equilibrium stage due to the low concentration of DB1 or MB in solution phase, as well as due to the less number of available adsorption sites onto composite gels.

The values of the intra-particle diffusion rate constants, derived from the slope of all three linear segments of q_t versus $t^{0.5}$ (Dogan, Ozdemir, & Alkan, 2007; Srivastava, Swamy, Mall, Prasad, & Mishra, 2006) (Fig. 7), are included in Table 4.

As Fig. 7 shows, the plots of q_t versus $t^{0.5}$ fail to pass through the origin. The deviation of straight lines from the origin (Fig. 7) may be due to the difference in rate of mass transfer in the initial (first linear segment, $k_{id,1}$) and final (third linear segment, $k_{id,3}$) stages of adsorption of the dyes onto composite hydrogels. The second linear segment is defined as a rate parameter ($k_{id,2}$), characteristic of the rate of adsorption in the region where intra-particle diffusion is rate-controlling step. Extrapolation of the second linear segment of the plots q_t versus $t^{0.5}$ back to the y-axis gives the intercepts, which provide information about the boundary layer thickness, the larger the value of the intercept, the greater the boundary layer diffusion effect is (Bayramoglu, Altintas, & Arica, 2009; Weber & Morris, 1963). As can be seen from Table 4, the values of the diffusion rate constant C_i are low, the highest value being found for the highest amount of the dye adsorbed (MB onto d-IPN2.60). This indicates an increase in thickness of the adsorbed layer and an effect of the boundary layer could be found only in this case. These results show that the adsorption process of DB1 and MB onto s-IPN1.60 and d-IPN2.60 composite hydrogels has a complex nature consisting of both physical adsorption and intra-particle diffusion, being influenced by both the gel and the dye structure.

Determining the best-fitting model is a key analysis to mathematically describe the involved sorption system and, therefore, to explore the related theoretical assumptions. In this study, two

Table 3
Kinetic data for the adsorption of ionic dyes on composite hydrogels.

Sample	Dye	$q_{e,exp}$ (mg/g)	Pseudo-first order constants				Pseudo-second order constants			
			$q_{e,calc}$ (mg/g)	k_1 (min^{-1})	R^2	χ^2	$q_{e,calc}$ (mg/g)	k_2 (g/mg min)	R^2	χ^2
s-IPN1.60	DB1	2.804	2.985	0.02	0.993	0.824×10^{-3}	3.902	0.5×10^{-2}	0.991	10.6×10^{-3}
d-IPN1.60	DB1	0.396	0.443	0.019	0.998	0.06×10^{-3}	0.618	2.5×10^{-2}	0.996	0.15×10^{-3}
s-IPN2.60	MB	0.392	0.377	0.04	0.970	0.05×10^{-3}	0.49	7.5×10^{-2}	0.978	0.07×10^{-3}
d-IPN2.60	MB	6.744	6.672	0.103	0.997	0.036×10^{-3}	7.285	2.56×10^{-2}	0.999	11.08×10^{-3}

Table 4
Intra-particle diffusion parameters for the adsorption of ionic dyes on composite hydrogels.

Sample	Dye	Intra-particle diffusion constants									
		$k_{id,1}$ (mg/g min$^{0.5}$)	R^2	χ^2	$k_{id,2}$ (mg/g min$^{0.5}$)	C_i	R^2	χ^2	$k_{id,3}$ (mg/g min$^{0.5}$)	R^2	χ^2
s-IPN1.60	DB1	0.476	0.990	0.07	0.246	0.074	0.993	0.18	0.016	0.852	0.091
d-IPN1.60	DB1	0.055	0.991	0.24	0.035	0.007	0.990	0.02	0.011	0.980	0.176
s-IPN2.60	MB	0.0701	0.898	0.05	0.042	0.01	0.989	0.01	0.021	0.960	0.158
d-IPN2.60	MB	2.013	0.903	0.31	0.756	3.858	0.920	0.40	0.038	0.958	0.13

statistical functions have been used to investigate their applicability as suitable tools to evaluate kinetic models fitness, namely the correlation coefficient of determination (R^2) and the non-linear Chi-square test (χ^2). The χ^2 test is basically the sum of the squares of the differences between the experimental data ($q_{e,exp}$, mg/g) and

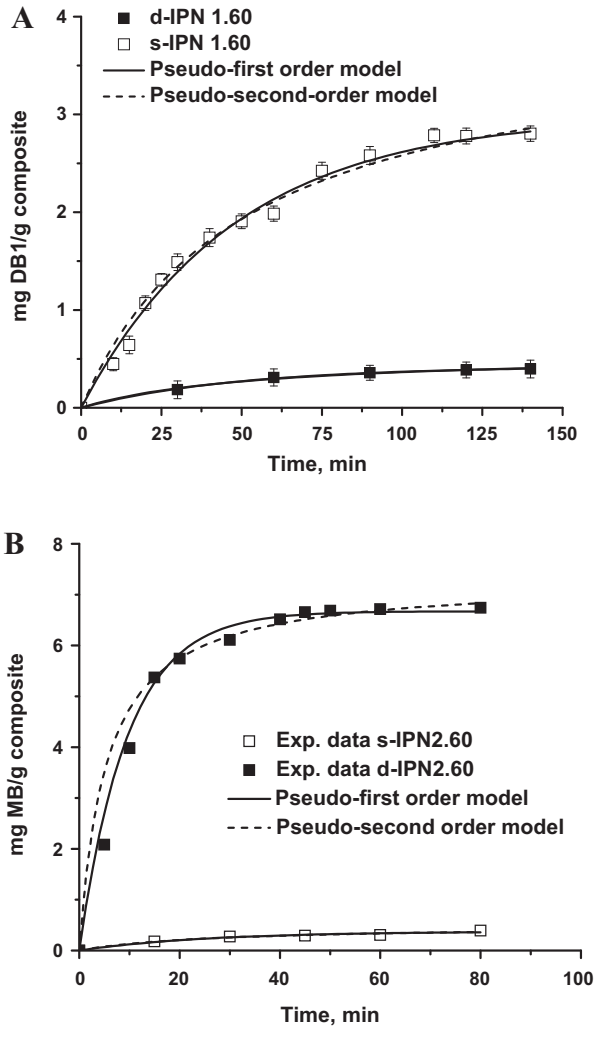

Fig. 6. Plots of q_t vs. t for DB1 adsorption onto d-IPN1.60 and s-IPN1.60 composite hydrogels (A), and for MB adsorption onto d-IPN2.60 and s-IPN2.60 (B).

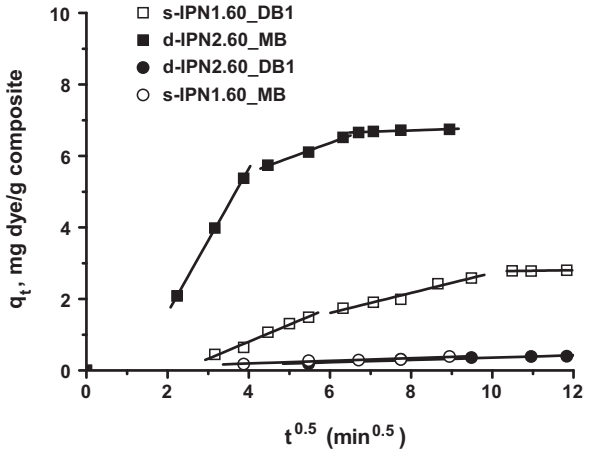

Fig. 7. Weber and Morris intra-particle diffusion plots for the dyes adsorption onto s-IPN1.60 and d-IPN2.60.

the data obtained by calculating from models ($q_{e,cal}$, mg/g), with each squared difference divided by the corresponding data calculated using the models, mathematically expressed by Eq. (9) (Ho & McKay, 1998):

$$\chi^2 = \sum \frac{(q_{e,exp} - q_{e,cal})^2}{q_{e,cal}} \quad (9)$$

If the data from a model are similar to the experimental data, χ^2 will be a small number, and if they strongly differ, χ^2 will be a big number. The results of the application of correlation coefficients (R^2) and χ^2 test on the experimental data of the equilibrium capacity ($q_{e,exp}$) for the all adsorption isotherms are shown in Tables 3 and 4. The pseudo-first order model appears to be the best fitting model for the sorption of dyes onto both composite hydrogels, with the highest correlation coefficient, and the lowest χ^2 values. Table 4 also indicates that the intra-particle diffusion model has the lowest correlation coefficients and higher χ^2 values comparative with those obtained for pseudo-first order model for all sorbents used in this study.

4. Conclusions

The preparation of s-IPN composite hydrogels as monoliths based on cross-linked PAAm as a matrix and CS as trapped polymer is described first in this paper. The influence of the ratio of cross-linker, pH of the reaction mixture, and CS molar mass on

the morphology of s-IPN composite hydrogels has been discussed based on the SEM analysis on the freeze dried samples. It was observed that with the increase of the cross-linker ratio, the pores were better defined, the morphology being the best preserved at the highest value of X ($X = 1/20$).

Full-IPN composite hydrogels have been prepared by a selective cross-linking with ECH of the CS chains trapped in s-IPN, in alkaline conditions. Formation of the second network strongly influenced not only the swelling ratio, but also the interaction of the composite gels with both anionic and cationic dyes. The explanation for the strong differences between s-IPN and d-IPN concerning the swelling and interaction with ionic dyes consists of the structural changes which occur during the formation of the second network at high pH, when part of the amide groups have been transformed in carboxylate groups by basic hydrolysis, thus generating an amphoteric IPN hydrogel, in one step. Analysis of the experimental kinetic data using pseudo-first order, pseudo-second order and intra-particle diffusion models revealed that the pseudo-first order kinetic was predominant for both dyes (DB1 and MB), the intra-particle diffusion being appropriate only for the sorption of DB1.

Acknowledgement

This work was supported by CNCSIS-UEFISCSU, by the project PNII-IDEI ID 981/2008.

References

Abd El-Rehim, H. A. (2006). Characterization and possible agricultural application of polyacrylamide/sodium alginate crosslinked hydrogels prepared by ionizing radiation. *Journal of Applied Polymer Science*, *101*, 3572–3580.

Agnihotri, S. A., & Aminabhavi, T. M. (2006). Novel interpenetrating network chitosan-poly(ethylene oxide-*g*-acrylamide) hydrogel microspheres for the controlled release of capecitabine. *International Journal of Pharmaceutics*, *324*, 103–115.

Bayramoglu, G., Altintas, B., & Arica, M. Y. (2009). Adsorption kinetics and thermodynamic parameters of cationic dyes from aqueous solutions by using a new strong cation exchange resin. *Chemical Engineering Journal*, *152*, 339–346.

Berger, J., Reist, M., Mayer, J. M., Felt, O., Peppas, N. A., & Gurny, R. (2004). Structure and interactions in covalently and ionically crosslinked chitosan hydrogels for biomedical applications. *European Journal of Pharmacy and Biopharmaceutics*, *57*, 19–34.

Brugnerotto, J., Lizardi, J., Goycoolea, F. M., Argüelles-Monal, W., Desbriéres, J., & Rinaudo, M. (2001). An infrared investigation in relation with chitin and chitosan characterization. *Polymer*, *42*, 3569–3580.

Byrne, M. E., & Salian, V. (2008). Molecular imprinting within hydrogels. II. Progress and analysis of the field. *International Journal of Pharmacy*, *364*, 188–212.

Cascone, M. G., Polacco, G., Lazzeri, L., & Barbani, N. (1997). Dextran/poly (acrylic acid) mixtures as miscible blends. *Journal of Applied Polymer Science*, *66*, 2089–2094.

Cestari, A. R., Vieira, E. F. S., dos Santos, A. G. P., Mota, J. A., & de Almeida, V. P. (2004). Adsorption of anionic dyes on chitosan beads. 1. The influence of the chemical structures of dyes and temperature on the adsorption kinetics. *Journal of Colloid and Interface Science*, *280*, 380–386.

Chen, J., Liu, M., & Chen, S. (2009). Synthesis and characterization of thermo- and pH-sensitive kappa-carrageenan-*g*-poly(methacrylic acid)/poly(N,N-diethylacrylamide) semi-IPN hydrogel. *Materials Chemistry and Physics*, *115*, 339–346.

Chung, A. J., & Rubner, M. F. (2002). Methods of loading and releasing low molecular weight cationic molecules in weak polyelectrolyte multilayer films. *Langmuir*, *18*, 1176–1183.

Dash, M., Chiellini, F., Ottenbrite, R. M., & Chiellini, E. (2011). Chitosan-A versatile semi-synthetic polymer in biomedical applications. *Progress in Polymer Science*, *36*, 981–1014.

Demirel, G., Özcetin, G., Şahin, F., Tümtürk, H., Aksoy, S., & Hasirci, N. (2006). Semi-interpenetrated polymer networks (IPNs) for entrapment of glucose isomerase. *Reactive and Functional Polymers*, *66*, 389–394.

Dhara, D., Nisha, C. K., & Chatterji, P. R. (1999). Superabsorbent hydrogels: Interpenetrating networks of poly(acrylamide-co-acrylic acid) and poly (vinyl alcohol): Swelling behavior and structural parameters. *Journal of Macromolecular Science: Pure and Applied Chemistry*, *A36*, 197–210.

Dinu, M. V., Perju, M. M., & Drăgan, E. S. (2011). Porous semi-interpenetrating hydrogel networks based on dextran and polyacrylamide with superfast responsiveness. *Macromolecular Chemistry and Physics*, *212*, 240–251.

Dogan, M., Ozdemir, Y., & Alkan, M. (2007). Adsorption kinetics and mechanism of cationic Methyl Violet and Methylene Blue dyes onto sepiolite. *Dyes and Pigments*, *75*, 701–713.

Domard, A. (1987). pH and c.d measurements on a fully deacetylated chitosan: Application to Cu^{II}–polymer interactions. *International Journal of Biological Macromolecules*, *9*, 98–104.

Franson, N. M., & Peppas, N. A. (1983). Influence of copolymer composition on non-Fickian water transport through glassy copolymers. *Journal of Applied Polymer Science*, *28*, 1299–1310.

Galaev, I. Y. (1995). Smart polymers in biotechnology and medicine. *Russian Chemical Reviews*, *64*, 471–489.

Gamzazade, A. I., Shimac, V. M., Skljar, A. M., Stykova, E. V., Pavlova, S. A., & Rogozin, S. V. (1985). Investigation of the hydrodynamic properties of chitosan solutions. *Acta Polymerica*, *36*, 420–424.

Hah, H. J., Kim, G., Lee, Y.-E. K., Orringer, D. A., Sagher, O., Philbert, M. A., et al. (2011). Methylene Blue-conjugated hydrogel nanoparticles and tumor-cell targeted photodynamic therapy. *Macromolecular Bioscience*, *11*, 90–99.

Ho, Y. S., & McKay, G. (1998). Sorption of dye from aqueous solution by peat. *Chemical Engineering Journal*, *70*, 115–124.

Hoare, T. R., & Kohane, D. S. (2008). Hydrogels in drug delivery: Progress and challenges. *Polymer*, *49*, 1993–2007.

Ilavsky, M., Hrouz, J., Stejskal, J., & Bouchal, K. (1984). Phase transition in swollen gels. 6. Effect of aging on the extent of hydrolysis of aqueous polyacrylamide solutions and on the collapse of gels. *Macromolecules*, *17*, 2868–2874.

Jeon, Y. S., Lei, J., & Kim, J. H. (2008). Dye adsorption characteristics of alginate/polyaspartate hydrogels. *Journal of Industrial and Engineering Chemistry*, *14*, 726–731.

Kim, B., La Flamme, K., & Peppas, N. A. (2003). Dynamic swelling behavior of pH-sensitive anionic hydrogels used for protein delivery. *Journal of Applied Polymer Science*, *86*, 1606–1613.

Kim, B., & Shin, Y. (2007). pH-sensitivity swelling and release behaviors of anionic hydrogels for intelligent drug delivery system. *Journal of Applied Polymer Science*, *105*, 3656–3661.

Kim, S. J., Yoon, S. G., Kim, I. Y., & Kim, S. I. (2004). Swelling characterization of the semi-interpenetrating polymer network hydrogels composed of chitosan and poly(diallyldimethylammonium chloride). *Journal of Applied Polymer Science*, *91*, 2876–2880.

Kumbar, S. G., Soppimath, K. S., & Aminabhavi, T. M. (2003). Synthesis and characterization of polyacrylamide-grafted chitosan hydrogel microspheres for the controlled release of indomethacin. *Journal of Applied Polymer Science*, *87*, 1525–1536.

Liang, S., Liu, L., Huang, Q., & Yam, K. L. (2009). Preparation of single or double-network chitosan/poly(vinyl alcohol) gel films through selective cross-linking method. *Carbohydrate Polymers*, *77*, 718–724.

Mandal, B. B., Kapoor, S., & Kundu, S. C. (2009). Silk fibroin/polyacrylamide semi-interpenetrating network hydrogels for controlled drug release. *Biomaterials*, *30*, 2826–2836.

Muzzarelli, R. A. A. (2009). Genipin-crosslinked chitosan hydrogels as biomedical and pharmaceutical aids. *Carbohydrate Polymers*, *77*, 1–9.

Myung, D., Waters, D., Wiseman, M., Duhamel, P. E., Noolandi, J., Ta, C. N., et al. (2008). Progress in the development of interpenetrating polymer network hydrogels. *Polymers for Advanced Technology*, *19*, 647–657.

Peppas, N. A., Hilt, J. Z., Khademhosseini, A., & Langer, R. (2006). Hydrogels in biology and medicine: From molecular principles to bionanotechnology. *Advanced Materials*, *18*, 1345–1360.

Ramesh Babu, V., Hosamani, K. M., & Aminabhavi, T. M. (2008). Preparation and in vitro release of chlorothiazide novel pH-sensitive chitosan-N,N′-dimethylacrylamide semi-interpenetrating network microspheres. *Carbohydrate Polymers*, *71*, 208–217.

Reis, A. V., Guilherme, M. R., Moia, T. A., Mattoso, L. H. C., Muniz, E. C., & Tambourgi, E. B. (2008). Synthesis and characterization of a starch-modified hydrogel as potential carrier for drug delivery system. *Journal of Polymer Science Part A: Polymer Chemistry*, *46*, 2567–2574.

Ritger, P. L., & Peppas, N. A. (1987). A simple equation to describe the solute release. II. Fickian and anomalous release from swellable devices. *Journal of Controlled Release*, *5*, 37–42.

Rodriguez, D. E., Romero-Garcia, J., Ramirez-Vargas, E., Ledezma-Perez, A. S., & Arias-Marin, E. (2006). Synthesis and swelling characteristics of semi-interpenetrating polymer network hydrogels composed of poly(acrylamide) and poly(γ-glutamic acid). *Materials Letters*, *60*, 1390–1393.

Rokhade, A. P., Patil, S. A., & Aminabhavi, T. M. (2007). Synthesis and characterization of semi-interpenetrating polymer network microspheres of acrylamide grafted dextran and chitosan for controlled release of acyclovir. *Carbohydrate Polymers*, *67*, 605–613.

Satish, C. S., Satish, K. P., & Shivakumar, H. G. (2006). Hydrogels as controlled drug delivery systems: Synthesis, crosslinking, water and drug transport mechanism. *Indian Journal of Pharmaceutical Sciences*, (March–April), 133–140.

Sperling, L. H. (1994). Interpenetrating polymer networks: An overview. In D. Klempner, L. H. Sperling, & L. A. Utracki (Eds.), *Interpenetrating polymer networks* (pp. 3–38). Washington: American Chemical Society.

Srivastava, V. C., Swamy, M. M., Mall, I. D., Prasad, B., & Mishra, I. M. (2006). Adsorptive removal of phenol by bagasse fly ash and activated carbon: Equilibrium, kinetics and thermodynamics. *Colloids and Surfaces A*, *272*, 89–104.

Tanaka, Y., Gong, J. P., & Osada, Y. (2005). Novel hydrogels with excellent mechanical performance. *Progress in Polymer Science*, *30*, 1–9.

Thierry, B., Winnik, F. M., Merhi, Y., Silver, J., & Tabrizian, M. (2003). Bioactive coatings of endovascular stents based on polyelectrolyte multilayers. *Biomacromolecules*, *4*, 1564–1571.

Varaprasad, K., Murali Mohan, Y., Ravindra, S., Narayana Reddy, N., Vimala, K., Monika, K., et al. (2010). Hydrogel–silver nanoparticle composites: A new generation of antimicrobials. *Journal of Applied Polymer Science*, *115*, 1199–1207.

Wan Ngah, W. S., Hanafiah, M. A. K. M., & Yong, S. S. (2008). Adsorption of humic acid from aqueous solutions on crosslinked chitosan-epichlorohydrin beads: Kinetics and isotherm studies. *Colloids and Surfaces B: Biointerfaces*, *65*, 18–24.

Wang, Q., Zhang, J., & Wang, A. (2011). pH-responsive carboxymethylcellulose-*g*-poly(sodium acrylate)/polyvinylpyrrolidone semi-IPN hydrogels with enhanced responsive and swelling properties. *Macromolecular Research*, *19*, 57–65.

Wang, T., Turhan, M., & Gunasekaran, S. (2004). Selected properties of pH-sensitive, biodegradable chitosan-poly(vinyl alcohol) hydrogel. *Polymer International*, *53*, 911–918.

Weber, W. J., Jr., & Morris, J. C. (1963). Kinetics of adsorption on carbon from solution. *Journal of the Sanitary Engineering Division: American Society of Chemical Engineering*, *89*, 31–59.

Xia, Y.-Q., Guo, T.-Y., Song, M.-D., Zhang, B.-H., & Zhang, B.-L. (2005). Hemoglobin recognition by imprinting in semi-interpenetrating polymer network hydrogel based on polyacrylamide and chitosan. *Biomacromolecules*, *6*, 2601–2606.

Yilmaz, Z., Kavakli Akkaş, P., Şen, M., & Güven, O. (2006). Removal of nitrite ions from aqueous solutions by poly(N,N-dimethylamino ethylmethacrylate) hydrogels. *Journal of Applied Polymer Science*, *102*, 6023–6027.

Zohuriaan-Mehr, M. J., Omidian, H., Doroudiani, S., & Kabiri, K. (2010). Advances in non-hygienic applications of superabsorbent hydrogel materials. *Journal of Materials Science*, *45*, 5711–5735.